UNCLASSIFIED

AD NUMBER
AD317134

CLASSIFICATION CHANGES

TO: **unclassified**

FROM: **confidential**

LIMITATION CHANGES

TO:

Approved for public release, distribution unlimited

FROM:

Distribution authorized to U.S. Gov't. agencies only; Administrative/Operational Use; 18 Jan 1960. Other requests shall be referred to the Office of Naval Research, 800 North Quincy Street, Arlingotn, VA 22217-5660.

AUTHORITY

ONR ltr, 31 Jan 1969; ONR ltr, 31 Jan 1969

THIS PAGE IS UNCLASSIFIED

UNCLASSIFIED

AD_ *3/7/34*

DEFENSE DOCUMENTATION CENTER

FOR

SCIENTIFIC AND TECHNICAL INFORMATION

CAMERON STATION ALEXANDRIA. VIRGINIA

CLASSIFICATION CHANGED
TO: UNCLASSIFIED_
FROM: CONFIDENTIAL_
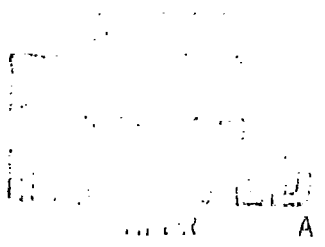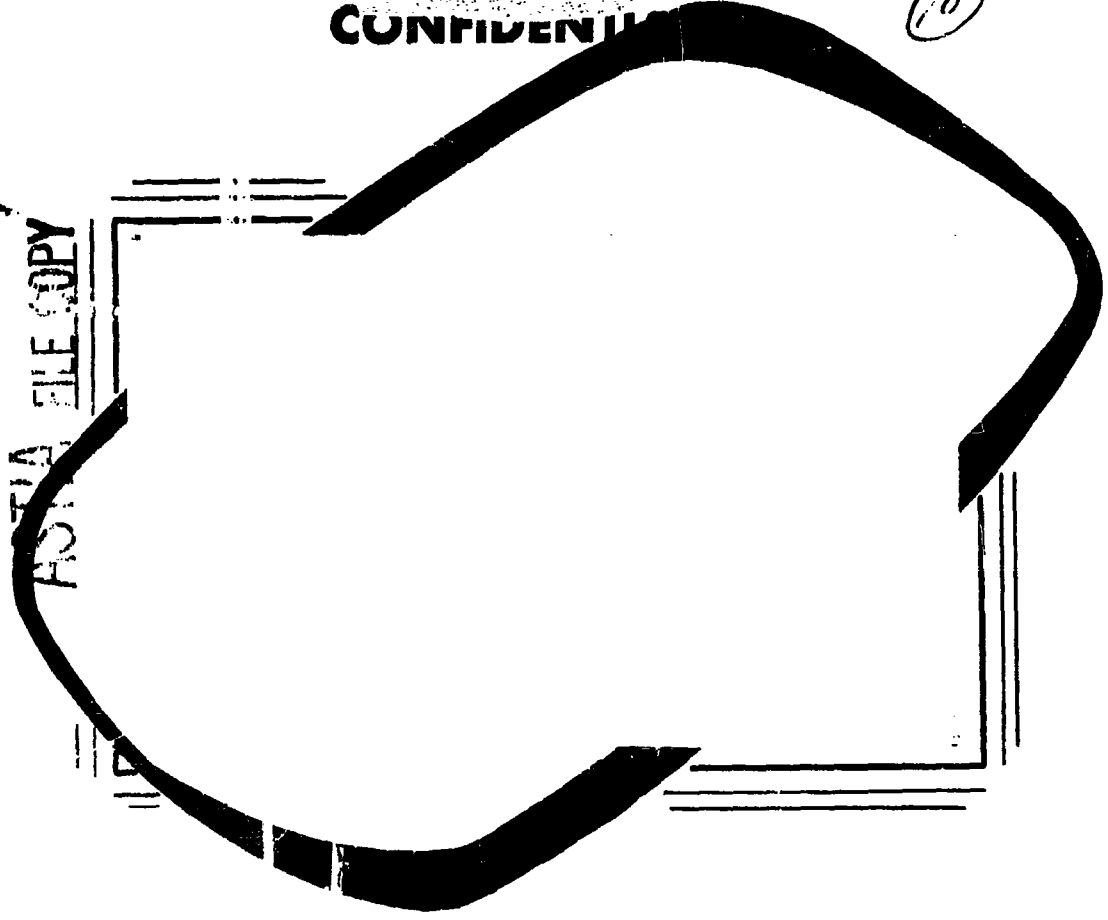AUTHORITY:
__ *CNR LeTTER*
__ *31 J AN. 69.*

UNCLASSIFIED

10

A

THE AEROPHYSICS DEPARTMENT
Of
MISSISSIPPI STATE UNIVERSITY

APPLICATION OF FULL SCALE
BOUNDARY LAYER MEASUREMENTS
TO DRAG REDUCTION OF AIRSHIPS

By

Joseph J. Cornish, III

&

Donald W. Boatwright

Research Report #28   18 January 1960

Conducted For

OFFICE OF NAVAL RESEARCH

Under

CONTRACT NONR 978 (02)

By

The Aerophysics Department

Mississippi State University

Reproduction in whole or in part is permitted
for any purpose of the United States Government

CONFIDENTIAL

TABLES AND FIGURES

DEFINITION OF SYMBOLS

U_∞ — Free Stream Velocity --feet per second or miles per hour

U — Velocity parallel to surface outside boundary layer

u — Velocity parallel to surface within boundary layer

δ^* — Boundary Layer Displacement Thickness--feet

$$\delta^* = \int_0^\delta \left(1 - \frac{u}{U}\right) dy$$

δ — Boundary Layer Thickness--feet. Height above surface where

$$u = 0.99 \, U$$

Θ — Boundary Layer Momentum Thickness--feet

$$\Theta = \int_0^\delta \frac{u}{U}\left(1 - \frac{u}{U}\right) dy$$

δ^{**} — Boundary Layer Energy Thickness--feet

$$\delta^{**} = \int_0 \frac{u}{U}\left(1 - \frac{u^2}{U^2}\right) dy$$

H — Boundary Layer Shape Parameter

$$H = \frac{\delta^*}{\Theta}$$

$\tilde{H}$ — Boundary Layer Energy Shape Parameter

$$H = \frac{\delta^{**}}{\Theta}$$

τ_0 — Skin Friction or Surface Shear--pounds per square foot

q — Local Dynamic Pressure--pounds per square foot

C_F — Overall Skin Friction Coefficient

C_f — Local Skin Friction Coefficient

Introduction

This report presents analyses of the drag and boundary layer characteristics of the ZS2G-1 airship as determined by full scale flight measurements of the boundary layer on the airship envelope and from total power requirements. These measurements were first made on the airship in its original service condition, and then were repeated after numerous protuberances, antennae, and fixtures were either removed or faired.

From the information obtained, the distribution of the drag among the airship component parts was determined and an estimate was made of the drag reduction possible by further modifications.

Experimental Apparatus and Test Procedures

The flight tests reported in this paper were conducted
on the U. S. Navy ZS2G-1 Airship Bu No. 240, in cooperation with
the AT & D division of the Naval Air Station at Lakehurst, New Jersey,
The test program was carried out in three phases, consisting first
of a preliminary investigation to qualitatively determine the extent
and the variation with airspeed of the areas of separated flow on
the airship envelope or bag. This was accomplished by attaching
approximately 2,200 Mylar tapes or tufts (Figure 1) to the after
portion of the envelope and to portions of the vertical fin and rudder.
These tufts were photographed at several airspeeds from a helicopter
flying alongside the airship. (Figure 2). The regions of separated
flow were then determined by detailed examinations of enlargements
of these photographs. A sketch of these areas is shown in Figure 3.
It was also possible from these photographs to determine roughly
the thickness of the boundary layer in the vicinity of the vertical
fin by examination of the behavior and condition of the tufts in
this region. The boundary layer thicknesses estimated by this
technique are also shown in Figure 3, and the entire phase is
reported in detail in Reference 1.

The second and third phases of the test program entailed the actual measurement of the boundary layer on the airship envelope and fin. For these measurements, three boundary layer rakes, two, five, and ten feet high, were constructed, these heights being estimated from theoretical calculations of the boundary layer on the envelope and from the tuft photographs. (Figure 4). The rakes were each equipped with 15 total head and 5 static pressure probes and were connected by means of multi-tube pressure tapes to a 20-tube water photomanometer with which the boundary layer profiles were recorded. Boundary layer profiles were measured at the 10, 20, 30, 40, 50, 60, 70, 80, 90, and 96 per cent stations on the envelope at airspeeds of 35, 40, 50, 60, and 70 miles per hour. The measurements were made along a sector of the envelope approximately 30° from the upper center line. To facilitate these measurements, the upper vertical fin was modified to accomodate two observers who occupied that position during flight. (Figure 5). Measurements of the boundary layer on the fin were made by probing at several locations from within the fin, with a pitot-static wand. The wand was calibrated to register distance from the fin surface, and the velocities were read directly on a Kollsman sensitive helicopter airspeed indicator.

These measurements were made on the airship in its original service condition and were repeated after the following modifications had been completed.

CONFIDENTIAL

1. Nose battens covered and faired with aircraft fabric.
2. ECM antennae and mountings removed.
3. Man-line along top of bag removed.
4. Navigation light cabling flush mounted.
5. AN/APS-38 radome removed and opening covered and faired.
6. Fuel and ballast dump faired in.
7. External hinges on car bottom made flush.
8. Jack pads removed.
9. APU air intake scoop removed.
10. Anti-collision light moved to top of upper vertical fin.
11. All finger patches faired with aircraft fabric.
12. All external catenary cables faired with aircraft fabric.
13. Fin brace cable attachments enclosed with Fiberglas fairings.
14. ART-13, ARR-15, and APN-70 antennae removed.
15. Sonar fish well covered and faired.
16. Shark fin antenna removed.

Approximately 24 flights, each lasting about 45 minutes, were required to complete the measurements. During each of the flights, the engine RPM and manifold pressure, the altitude, and carburettor air temperature, and the airship angle of attack and heaviness were recorded in order to determine the brake horsepower required at each test condition.

Results and Analysis of Data

From the flight test data it was possible to determine the distribution of local velocity along the length of the airship. Figure 6 shows the local velocity distributions measured in the original and modified conditions at the airspeeds tested. These data agree well with the analyses of the tuft tests, (Figure 3), which indicate that flow separation does not occur until far back on the bag. The pressure recovery, as shown by the velocity distribution, indicates that the flow remains well attached far aft on the envelope. The good pressure recovery suggests that the drag of the envelope is mainly due to skin friction rather than pressure drag. This premise is substantiated by the boundary layer measurements.

Figure 7 shows typical boundary layer developments along the bag for the original and the modified conditions. A theoretical boundary layer development due to Millikan (Reference 2) is also shown for comparison. The thinner boundary layer in the modified condition is due to the fairing of the rough, exposed battens at the nose of the airship. It can be seen that the measured boundary layer development closely follows the growth predicted for the ideal theoretical case increasing to a thickness of 10 feet at the 96 per cent station. Two typical boundary layer profiles

of the 100 profiles measured in the original and in the modified
conditions.are shown in Figure 8. All measured boundary layer
profiles were reduced to yield the conventional parameters,
$\delta^*, \Theta, \delta^{**}, H$, and two typical distributions of these
parameters are presented in Figure 9. It is of interest to note
the relatively low values of the parameter H. For boundary
layers not near separation with Reynolds Numbers, R_Θ, of the
order of 100 to 1,000, H is generally of the order of 1.4 to 1.5.
However, at the higher Reynolds Numbers of the present tests,
the values of H are seen to vary from 1.2 to 1.3.

From the measured profiles, it was also possible to
determine the local skin friction coefficient C_f, utilizing a form
of the Ludweig-Tillman wall law. An example of this distribution
is shown in Figure 10, for both the modified and original conditions.
The skin friction distributions also show that the flow remains
unseparated until well beyond the 90 per cent station, giving a
low pressure drag as indicated by the tuft photos and the pressure
distributions.

These distributions of local properties of the boundary
layer can be integrated over the envelope surface to give overall
coefficients for the entire envelope. Figure 11 shows the variation
with airspeed of the envelope skin friction drag before and after
fairing the nose battens. The skin friction coefficients presented

in this figure are based on the volume of the airship to the two-thirds power, as are all non-dimensional coefficients in this report, and represent the contribution of skin friction to the total drag of the envelope. In addition to the skin friction drag, the envelope total drag was determined by examinations of the envelope wake as deduced from the boundary layer measurements. The development of the boundary layer and the envelope wake for a typical case is shown in Figure 12. The wakes determined in this manner were then integrated to yield total envelope drag and these values, reduced to coefficient form are given in Figure 13, as a function of airspeed. A comparison of these values of total drag coefficients and the skin friction coefficients of Figure 11 reveals that, within the experimental scatter, there is a little apparent difference, indicating a very low pressure drag for the envelope.

These measurements on the airship envelope were used to determine the drag and horsepower requirements for the envelope as a function of airspeed and are presented in Figure 14. Also shown in this figure are the brake horsepower and thrust horsepower required for the entire airship. These data were obtained from the engine information gathered in flight. The thrust horsepower was obtained using the brake horsepower and a propeller efficiency of 66 per cent. This value was taken from Reference 3, as being representative of the ZS2G-1 engine-propeller installations.

From these two curves, the thrust horsepower and the total envelope drag, the aggregate drag of the remaining airship components, eg., the fins, car, engines, was calculated. This drag increment was apportioned among the various components. Table 1 shows several such drag breakdowns for the ZS2G-1 airship. The first column of the table is the drag breakdown of this airship as reported in Reference 3, and is presumably typical of the airship in service condition. The figures are presented as percentages, taking the total airship drag as 100 per cent. Column 2 of the table shows a drag breakdown of the airship based upon the present measurements on the envelope in its original condition and upon the measurements of total airship power required. In this breakdown, the envelope drag has been subtracted from the total drag and the difference distributed among the various remaining components. The increments for each component were distributed in the same proportions as in Column 1 of the table. Column 2, based upon flight tests, shows a somewhat lower percentage drag for the envelope.

Column 3 shows the drag breakdown for the airship after the previously listed modifications had been made. These figures were also computed using the original total airship drag as a reference of 100 per cent. These measurements indicated that the modified airship had 77. 6 per cent of the original total drag, and that the percentage envelope drag had been reduced from 44. 6

per cent to 35. 2 per cent of the original total drag. In distributing
the drag among the remaining components, the amount of modifi-
cation to each component was taken into account. Those items
which were unaltered retained their original percentage drag,
while the drag of any modified component was reduced accordingly.

Discussion of Results and Projected Research

As a result of these investigations, some of the fundamental
properties of the flow in the boundary layer at very high Reynolds
Numbers have been disclosed. While there is a wealth of infor-
mation at high Reynolds Numbers, the data is generally obtained
at relatively high Mach Numbers and includes the effects of com-
pressibility. The present data, however, has been taken at low
speed and very large boundary layer thick..esses and provides
information applicable throughout the incompressible flow regime.
For example, the present data can be readily applied to bodies
submerged in water.

The importance of maintaining smooth, faired surfaces even
at these very large boundary layer thicknesses is obvious. By
covering and smoothing the battens at the nose of the airship,
the drag of the envelope was reduced to 79 per cent of its original
value. It is of interest to note that the reduction in envelope

drag resulted mainly from a decrease in the local skin friction. The pressure drag was found to be a small factor in the total drag as compared to the skin friction. A comparison of the total drag variation with airspeed and the skin friction variation with airspeed shows that the total drag varies in the same manner as the skin friction, except at the lower speeds tested. At the lower speeds, the total drag drops off with airspeed more rapidly than the skin friction, indicating that the pressure drag decreases sharply with airspeed until it becomes a small part of the total drag. This observation is substantiated by the tuft photographs which show that the region of separated flow decreases more rapidly at the lower airspeeds.

The lower values of the shape parameter H are commensurate with the high Reynolds Numbers of the tests. A measure of the effectiveness of accelerating the wake of this airship can be found using the shape parameter $\overline{H}$. The principle of wake acceleration is based upon the fact that it is more economical, powerwise, to reaccelerate the slowed down wake to obtain a given thrust than it is to obtain this same thrust from a propeller operating in the freestream flow. (Reference 4). If it is assumed that the pressure drag is negligible, as is true in the present case, the ratio of these powers required can be shown to be:

$$\frac{HP_{Wake\ Accel.}}{HP_{Free\ Stream}} = \frac{\delta^{**}}{2\theta} = \frac{\bar{H}}{2}$$

Figure 15 shows the percentage power savings which could be expected from re-accelerating the airship wake. It can be seen that this saving amounts to approximately 10 per cent of the power required throughout the range of airspeed tests, and in general, shows a decreasing trend with increasing airspeed.

The modifications to the airship completed during the present tests have resulted in a 22.4 per cent reduction in total drag. Additional modifications, which are now in progress, are expected to still further reduce the total drag. A tension field fillet is to be installed at the base of each of the fins and additional fairings placed over protuberances still remaining on the fin surfaces. These modifications are expected to result in an additional 3 per cent to 5 per cent reduction in the total drag. However, the more important effect of these modifications will be the improvement of the flow over the fin and rudder surfaces giving better control and stability. As indicated by the tuft pictures, there exists an extensive region of low velocity flow over the fins and rudders. The results of the boundary layer measurements on the

upper vertical fin are shown in Figure 16. The data is presented as lines of equal boundary layer momentum loss by plotting Θ, over the surface of the fin. The extent to which the fin is immersed in the low velocity flow near the envelope is also indicated by the thickness of the envelope boundary layer. Of particular interest is the adverse effect of the fin fittings and brace cable attachments. It can be seen that these disturbances cause considerable momentum losses to the downstream boundary layer. The effects of this low momentum flow which lower the effectiveness of the fin and rudder can be minimized by suitable additional fairings to the disturbances.

It is of further interest, however, to examine the effects of more extensive modifications to the airship aimed at greatly improving its range and controlability. These modifications would include the installation of a stern propulsion system on the airship which would provide both thrust and control. Figure 17 shows a sketch of such an installation. The stern-mounted engine would power a helicopter rotor which, by means of its cyclic pitch controls, would supply the turning moments necessary to maneuver the airship. This system would allow the removal of existing fins and rudders as well as the existing engines and nacelles. For preliminary tests, however, the presently installed engines could be left intact.

Column 4 of Table I gives the estimated drag breakdown of a stern propelled ZS2G-1 airship with faired nose battens, tail surfaces removed, and envelope, tail surface, and engine car braces removed. Some residual tail surface and tail surface brace drag has been included to account for a partial span fin mounted vertically beneath the envelope to serve as protection for the helicopter rotor during high angle landings. It is seen that these modifications reduce the drag to about 64 per cent of the original unmodified airship.

The next column, Number 5, itemizes the component drag of an advanced ZS2G-1 with stern propulsion. In this case, the envelope drag has been reduced by completely smoothing the battens and envelope. The anal fin has been replaced with a retractable skid having only 30 per cent of the drag of the fin, and eliminating the remaining tail surface braces. The control lines have been made flush, thus eliminating their drag. In the light of past work in drag reduction, e. g. , reference 6, where the drag of a comparatively clean Beech L-23 was reduced to 60 per cent of its original value, it is felt that the car drag could be reduced to 58 per cent of its present value. The outriggers and nacelles are removed, thus eliminating their drag and by retracting the handling lines, their drag is removed. These further modifications reduce the drag of the airship to 43 per cent of its original value. This vastly improved airship would greatly extend the range and operating capabilities of present airship techniques.

CONFIDENTIAL

Concluding Remarks

The data obtained during the present flight tests of the ZS2G-1 airship have revealed several fundamental characteristics:

1. The drag of the airship is almost evenly divided between the airship envelope and the remaining airship components.

2. The envelope drag is mainly due to skin friction rather than pressure drag.

3. The pressure drag coefficient, as well as the skin friction coefficient, decreases with increasing Reynolds numbers.

4. By suitable modifications to the nose of the airship, the overall skin friction of the envelope has been reduced by more than 20 per cent.

5. Performance estimates based on present data show that the total airship drag can be reduced to 42 per cent of its present value by a bold modification using a helicopter rotor for propulsion and control.

REFERENCES

1. "Tuft Flow Studies on ZS2G-1 Type Airship," (Confidential), Cornish, J. J., III, and Boatwright, D. W., Research Note #6, Aerophysics Department, Mississippi State University, 10 June 1959.

2. "The Boundary Layer and Skin Friction for a Figure of Revolution," Millikan, C. B., ASME Transactions 1932, Volume 54, p. APM-54-3 vo.

3. "Performance Estimates for the XZP5K Airship," Goodyear Aircraft Corporation, G. E. R. 5268, May 1953.

4. "Wake Stream Acceleration as Means for Reducing Airplane Drag," Burgdorfer, A., Escher Wyss, Technical Note #1, July 1956.

5. "Performance Improvement on YL-23, Second Series," Raspet, August, Research Report #12, Aerophysics Department, Mississippi State University, November 1957.

CONFIDENTIAL

TABLE I

PERCENT DRAG BREAKDOWN FOR VARIOUS AIRSHIP CONFIGURATIONS

|	I	II	III	IV	V
	ZS2G-1 #	ZS2G-1 *	Modified * ZS2G-1	Stern Propelled Airship	Advanced Stern Propelled Airship
Envelope	51.20	44.60	35.20	35.00	30.00
Envelope accessories	1.34	1.40			
Tail surfaces	11.50	13.08	9.46	2.18	0.80
Tail surface brace cables	7.85	8.90	7.00	0.99	
Control lines	1.59	1.80	1.80	1.80	
Tail surface accessories	0.46	0.52			
Control car	9.00	10.23	7.73	7.73	6.00
Outriggers	2.67	3.07	3.07	3.07	
Nacelles	4.52	5.15	5.15	5.15	
Cooling drag	5.39	6.13	6.13	6.13	6.13
Car & engine accessories	1.80	2.06			
Handling lines	1.34	1.53	1.53	1.53	
Misc. & interference	1.34	1.53	0.53	0.51	0.20
Total	100.00	100.00	77.60	64.09	43.13

\# GER 5268

* Present Measurements

CONFIDENTIAL
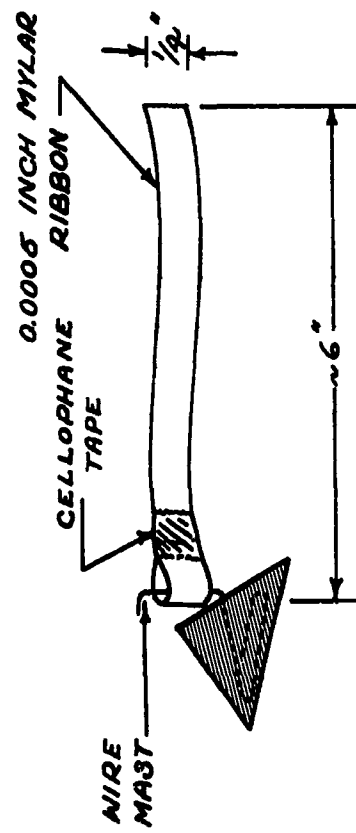
FIGURE 1

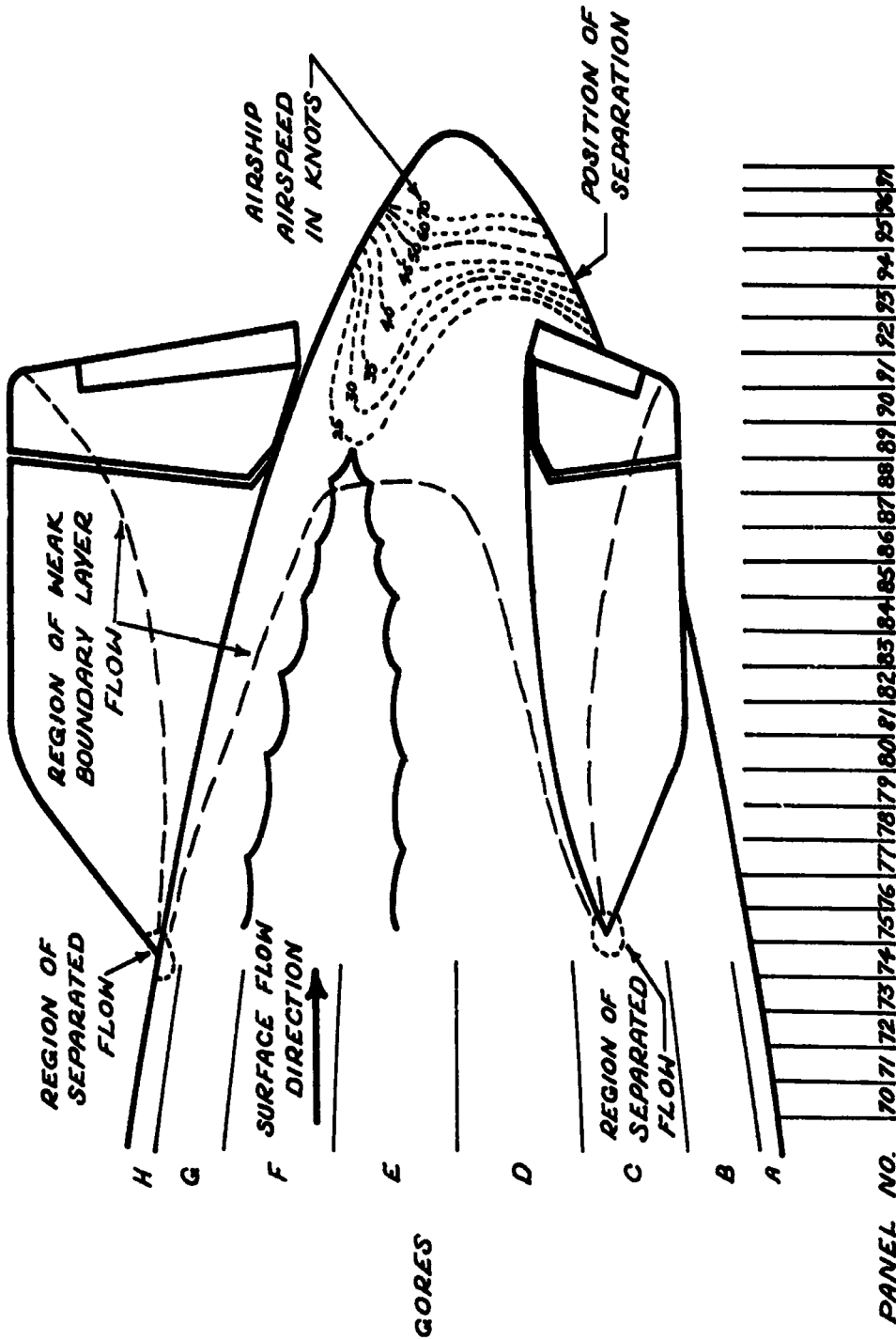SKETCH OF TUFT DEVELOPED FOR AIRSHIP
BOUNDARY LAYER RESEARCH

0.0005 INCH MYLAR RIBBON

CELLOPHANE TAPE

WIRE MAST

½"

~6"

FIGURE 2

PHOTOGRAPH OF TUFTS ON ZS2G-1 AIRSHIP

FIGURE 3

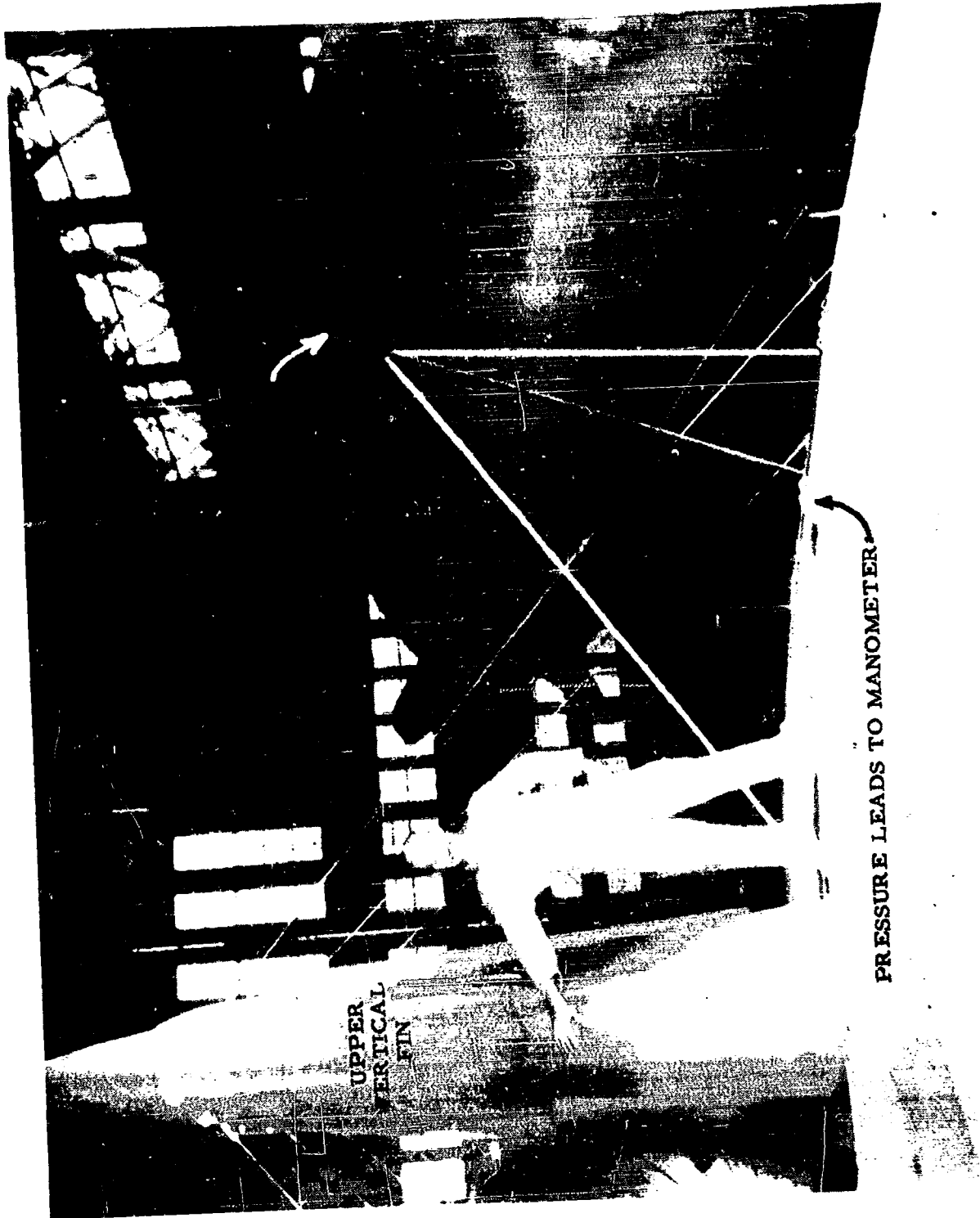SEPARATION REGION ON ZS2G-1 AIRSHIP
STRAIGHT AND LEVEL FLIGHT

FIGURE 4

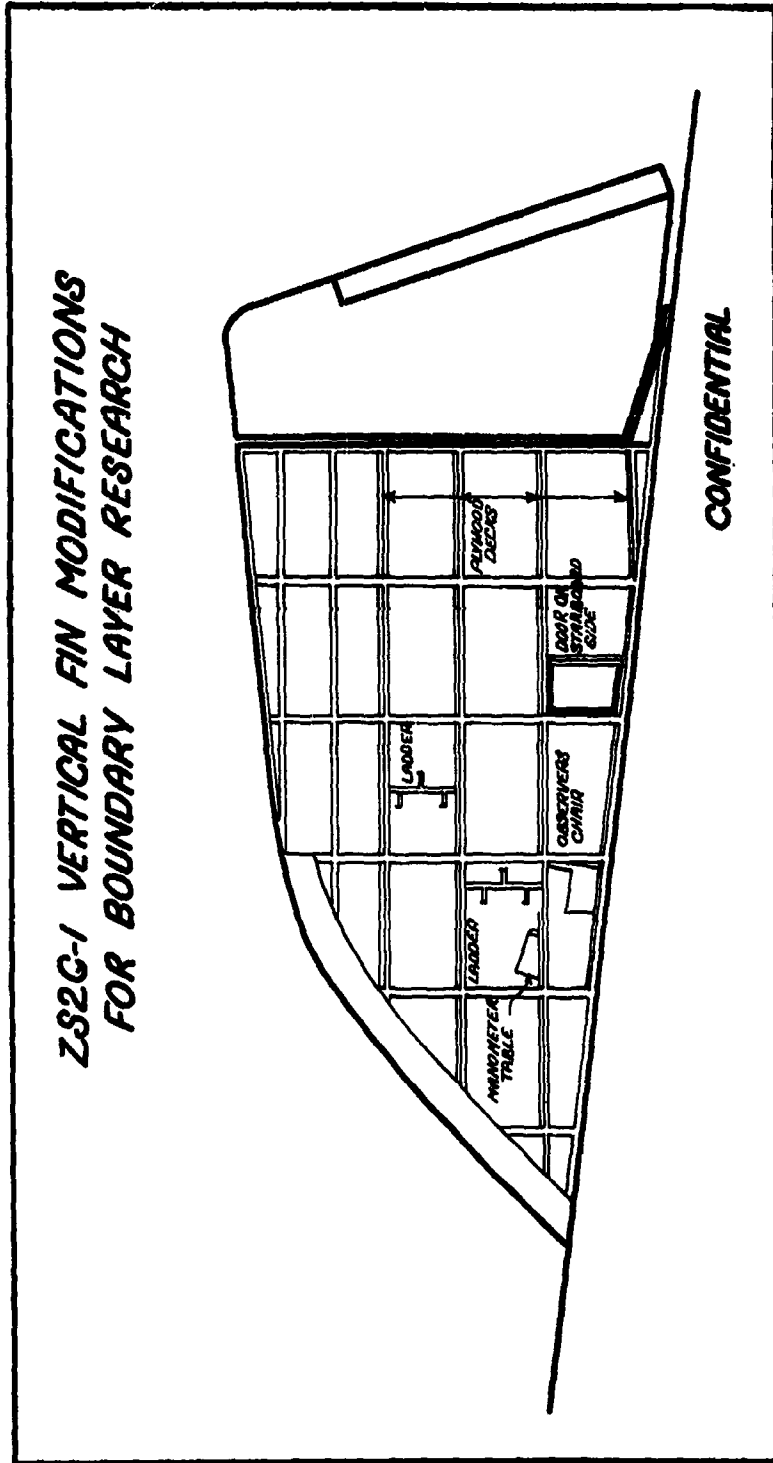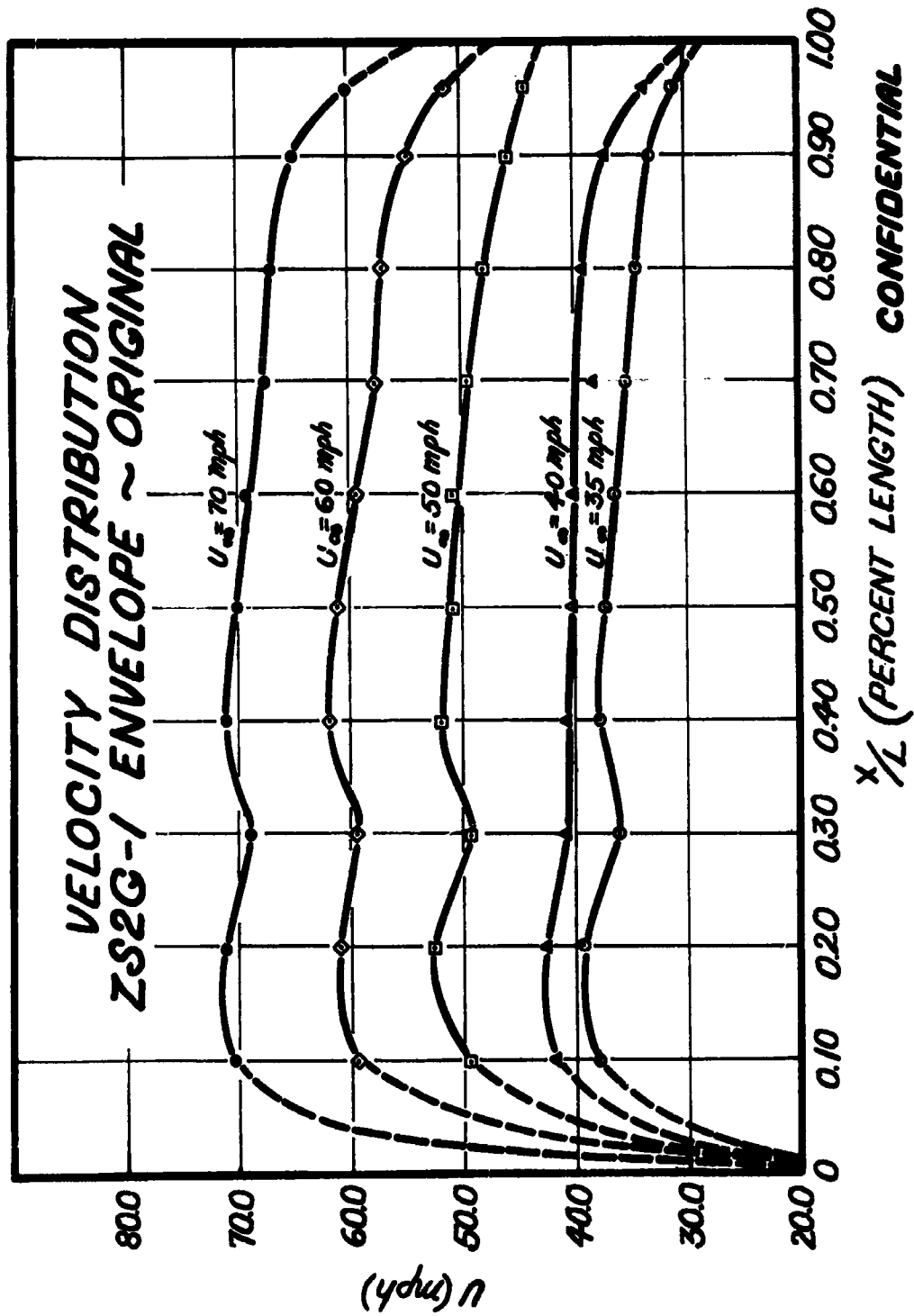PRESSURE LEADS TO MANOMETER

UPPER VERTICAL FIN

FIGURE 5

ZS2C-I VERTICAL FIN MODIFICATIONS FOR BOUNDARY LAYER RESEARCH

CONFIDENTIAL

VELOCITY DISTRIBUTION
ZS2G-1 ENVELOPE ~ ORIGINAL

$U_o = 70\ mph$

$U_o = 60\ mph$

$U_o = 50\ mph$

$U_o = 40\ mph$

$U_o = 35\ mph$

x/L (PERCENT LENGTH)

U (mph)

CONFIDENTIAL

VELOCITY DISTRIBUTION
ZS2G-1 ENVELOPE ~ MODIFIED

U_∞ = 70 mph

U_∞ = 60 mph

U_∞ = 50 mph

U_∞ = 40 mph

U_∞ = 35 mph

x/L (PERCENT LENGTH)   CONFIDENTIAL

u (mph)

FIGURE 7

BOUNDARY LAYER COMPARISON
ZS2G-I ENVELOPE

○ XZP5K ● 80 KNOTS (THEORETICAL)
▲ ZS2G-I @ 70 mph (ORIGINAL CONDITIONS)
◘ ZS2G-I @ 70 mph (MODIFIED)

X/L (PERCENT LENGTH) CONFIDENTIAL

S ~ (BOUNDARY LAYER THICKNESS IN FEET)

FIGURE 8

TYPICAL BOUNDARY
LAYER PROFILES
70% STATION
$U_\infty = 70\ mph$

$S_{ORIGINAL}$

$S_{MODIFIED}$

⊙ ORIGINAL CONDITION
⊡ MODIFIED CONDITION

$Y_{IN.}$

$\dfrac{u}{U}$

CONFIDENTIAL

BOUNDARY LAYER PARAMETERS
ZS2G-I ENVELOPE
ORIGINAL CONDITION ~ 70 mph

H (BOUNDARY LAYER SHAPE PARAMETER)

x/L (PERCENT LENGTH)   CONFIDENTIAL

S*, θ, S** (INCHES)

BOUNDARY LAYER PARAMETERS
ZS2G-1 ENVELOPE
MODIFIED CONDITION ~ 70 mph

H (BOUNDARY LAYER SHAPE PARAMETER)

$\frac{x}{L}$ (PERCENT LENGTH)

S^*, θ, S^{**} (INCHES)

CONFIDENTIAL

FIGURE 10

LOCAL SKIN FRICTION COEFFICIENT
ZS2G-1 ENVELOPE ~ U∞ = 70 mph

• ORIGINAL CONDITION
▪ MODIFIED CONDITION

x/L (PERCENT LENGTH) CONFIDENTIAL

C_f

FIGURE 11

OVERALL SKIN FRICTION COEFFICIENT
ZS2G-1 ENVELOPE

• ORIGINAL CONDITION
• MODIFIED CONDITION

C_f

$u_\infty \sim mph$

CONFIDENTIAL

FIGURE 12

WAKE OF ZS2G-1 EXTRAPOLATED FROM BOUNDARY MEASUREMENTS

FLIGHT VELOCITY = 35 mph

CONFIDENTIAL

FIGURE 13

ENVELOPE TOTAL DRAG COEFFICIENT
VERSUS AIRSPEED ~ ZS2G-1 AIRSHIP

○ ORIGINAL CONDITION
□ MODIFIED CONDITION

U_∞ ~ mph

ENVELOPE TOTAL DRAG COEFFICIENT ~ C_{D_t}

FIGURE 14

POWER REQUIREMENTS
ORIGINAL AND MODIFIED ~ZS2G-1

- ORIGINAL CONDITION
- MODIFIED CONDITION

BHP

THP

ENVELOPE

HORSEPOWER REQUIRED

$U_\infty \sim mph$

CONFIDENTIAL

PERCENT POWER SAVING WITH WAKE ACCELERATION ~ ZS2G-I AIRSHIP

FIGURE 15

FIGURE 16

MOMENTUM THICKNESS IN INCHES
VERTICAL FIN OF ZS2G-1 AIRSHIP ~ 70 mph

CONFIDENTIAL